Published in final edited form as:
J Neurosci. 2000 February 1; 20(3): 929–936.

Somatostatin Modulates Voltage-Gated K^+ and Ca^{2+} Currents in Rod and Cone Photoreceptors of the Salamander Retina

Abram Akopian[1], **Juliette Johnson**[3], **Robert Gabriel**[1], **Nicholas Brecha**[3,4,5], and **Paul Witkovsky**[1,2]

[1] Department of Ophthalmology, New York University School of Medicine, New York, New York 10016

[2] Department of Physiology and Neuroscience, New York University School of Medicine, New York, New York 10016

[3] Department of Neurobiology, University of California, Los Angeles, School of Medicine, Los Angeles, California 90095

[4] Department of Medicine, Jules Stein Eye Institute and Center for Ulcer Research and Education, Division of Digestive Diseases, University of California, Los Angeles, School of Medicine, Los Angeles, California 90095

[5] Veterans Administration Medical Center-West Los Angeles, Los Angeles, California 90073

Abstract

We investigated the cellular localization in the salamander retina of one of the somatostatin [or somatotropin release-inhibiting factor (SRIF)] receptors, sst_{2A}, and studied the modulatory action of SRIF on voltage-gated K^+ and Ca^{2+} currents in rod and cone photoreceptors. SRIF immunostaining was observed in widely spaced amacrine cells, whose perikarya are at the border of the inner nuclear layer and inner plexiform layer. sst_{2A} immunostaining was seen in the inner segments and terminals of rod and cone photoreceptors. Additional sst_{2A} immunoreactivity was expressed by presumed bipolar and amacrine cells. SRIF, at concentrations of 100–500 nM, enhanced a delayed outwardly rectifying K^+ current (I_K) in both rod and cone photoreceptors. SRIF action was blocked in cells pretreated with pertussis toxin (PTX) and was substantially reduced by intracellular $GDP_\beta S$. Voltage-gated L-type Ca^{2+} currents in rods and cones were differently modulated by SRIF. SRIF reduced Ca^{2+} current in rods by 33% but increased it in cones by 40%, on average. Both effects were mediated via G-protein activation and blocked by PTX. Ca^{2+}-imaging experiments supported these results by showing that 500 nM SRIF reduced a K^+-induced increase in intracellular Ca^{2+} in rod photoreceptor terminals but increased it in those of cones. Our results suggest that SRIF may play a role in the regulation of glutamate transmitter release from photoreceptors via modulation of voltage-gated K^+ and Ca^{2+} currents.

Keywords

somatostatin; retina; Ca^{2+} channel; K^+ channel; G-protein; patch clamp

Somatostatin, also called somatotropin release-inhibiting factor (SRIF), initially was identified as a hypothalamic peptide but subsequently has been shown to be widely distributed in the nervous system and in peripheral endocrine organs (Delfs and Dichter,

Correspondence should be addressed to Dr. Abram Akopian, New York University School of Medicine, 550 First Avenue, New York, NY 10016. aa3@is4.nyu.edu.

1985). The cellular actions of SRIF are mediated via five distinct G-protein-coupled receptors, $sst_{1–5}$ (Hoyer et al., 1995). In addition, there are two sst_2 isoforms resulting from alternative mRNA splicing (Vanetti et al., 1992). SRIF has been shown to modulate K^+ and Ca^{2+} currents in neurons, endocrine cells, and some cell lines. Many classes of K^+ current are reported to be increased by SRIF, including a K^+ leak current (Schweitzer et al., 1998), an inward rectifier (Takano et al., 1997), a delayed rectifier K^+ current (Wang et al., 1989), and a Ca-activated K^+ current (White et al., 1991). The effect of SRIF on Ca current is inhibitory, and it acts on high voltage-activated Ca^{2+} currents of the L-type (Rosenthal et al., 1988) and N-type (Shapiro and Hille, 1993). In axonal terminals, the combined action of SRIF on K^+ and Ca^{2+} currents has been reported to reduce transmitter release (Katayama and Hirai, 1989; Boehm and Betz, 1997).

In the vertebrate retina, SRIF-containing neurons typically are amacrine (Yamada et al., 1980; Li and Lam, 1990; Rickman et al., 1996) or interplexiform cells (Smiley and Basinger, 1988). SRIF-immunoreactive fibers are predominantly distributed to selected laminae of the inner plexiform layer (IPL). Physiological data on the role of SRIF in retinal function, however, are scant. Zalutsky and Miller (1990) reported that SRIF was excitatory to most ganglion cells tested in rabbit retina, but whether the peptide acted directly on ganglion cells or via circuitry that is presynaptic to ganglion cells was not determined. More recently, sst_{2A} immunostaining was localized to a variety of rat and rabbit retinal neurons, including bipolar cells and cone photoreceptors (Johnson et al., 1998, 2000). The location of sst_{2A} receptors on photoreceptor terminals suggested a possible role of SRIF in regulating the release of glutamate, the identified neurotransmitter of photoreceptors (Marc et al., 1990; for review, see Thoreson and Witkovsky, 1999).

In the present study we examined the action of SRIF on rod and cone photoreceptor terminals in the salamander retina. We showed, by immunocytochemistry, that in the salamander retina, both rods and cones express sst_{2A} receptors. Using the whole-cell patch-clamp technique, we found that SRIF had a differential action on the high voltage-activated L-type Ca^{2+} currents of rods and cone inner segments; it reduced the Ca^{2+} current of rods but increased that of cones. In addition, SRIF increased the delayed rectifier K^+ current of rods and cones. These data suggest that, like dopamine (for review, see Witkovsky and Dearry, 1991), SRIF may play a role in governing the balance of information flow through rod and cone circuits.

MATERIALS AND METHODS

Animals

Salamanders (*Ambystoma tigrinum*) were obtained from a commercial supplier (Charles Sullivan, Nashville, TN) and kept at 4°C until used. The handling and maintenance of animals met the National Institutes of Health guidelines and were approved by the animal research committees of New York University School of Medicine and University of California, Los Angeles, School of Medicine (UCLA).

Tissue preparation for immunohistochemical experiments

After decapitation, the eyes were removed, the anterior segment was dissected away, and the posterior eyecup containing the retina was immediately immersed in 4% paraformaldehyde (PFA) in 0.1 M phosphate buffer (PB). The eyecup was fixed for 1 hr at room temperature and then stored in 25% sucrose in 0.1 M PB at 4°C. Vertical sections of the retina were cut perpendicular to the vitreal surface with a cryostat at 12–16 μm, mounted onto gelatin-coated slides, and then air-dried and stored at −20°C.

Cell isolation procedure

The retinas were removed from the salamander eyecups, exposed to 20 U/mg papain (Worthington, Freehold, NJ) for 30 min, and then washed several times with Ringer's solution [composition (in mM), NaCl 100; KCl 2.5; $CaCl_2$ 1.8; $MgCl_2$ 1.0; and $NaHCO_3$ 25, pH 7.4]. The remaining procedures for cell isolation are identical to those reported previously (Akopian and Witkovsky, 1996). Dissociated cells were plated onto concanavalin A (Sigma, St. Louis, MO)-coated coverslips. Isolated cells were used in immunocytochemical and Ca^{2+}-imaging experiments. For immunocytochemical experiments, cells were fixed in 4% PFA for 10 min followed by three washes with 0.1 M PB.

Antibodies

The SRIF antibody and the tyrosine hydroxylase monoclonal mouse antibody were obtained from Chemicon (Temecula, CA). A rabbit affinity-purified polyclonal antibody (#9431) directed against the C terminus of mouse sst_{2A} 361–369 was a generous gift of Drs. J. Walsh and Helen Wong of UCLA. After a blocking step in an antibody diluent solution, the primary antibodies were placed on the tissues or isolated cells for 12–36 hr at 4°C and then washed in 0.1 M PB. The immunoreaction was visualized with fluorescein-isothiocyanate-coupled goat anti-rabbit antibodies (American Qualex, La Mirada, CA) or rhodamine donkey anti-mouse (Jackson ImmunoResearch, West Grove, PA) for 1–2 hr at room temperature. Sections were coverslipped with a glycerol phosphate or carbonate buffer containing 2% potassium iodide to retard fading.

The specificity of the sst_{2A} antibody was evaluated by preadsorbing it with 10^{-5} M synthetic sst_{2A} peptide, which completely abolished labeling. In addition, the sst_{2A} antiserum has been characterized extensively in a previous study using transfected cell lines, Western blotting, and immunohistochemistry on tissue sections (Sternini et al., 1997).

Image processing

Images were photographed using T-Max 400 or Ektachrome 1600 film. The photographic images were scanned at 2700 dpi with a SprintScan 35/Plus scanner (Polaroid, Cambridge, MA) and saved as TIFF files. Images were adjusted to the final size, corrected for contrast and brightness, and labeled using Adobe Photoshop 5.0 (Adobe Systems, Mountain View, CA). Images were saved at 320 dpi.

Ca^{2+} imaging

Retinal cells were isolated, incubated for 10–15 min at room temperature in darkness with the membrane-permeable fluorescent dye fura-2 AM (Molecular Probes, Eugene, OR) at a concentration of 5–10 μM, and then washed in Ringer's solution. Rods and cones were identified by their characteristic morphology. A coverslip with the cells was transferred to a stage mounted on a Zeiss 135 Axiovert inverted microscope on which the cells were superfused with Ringer's solution containing either 50 or 100 mM K^+ alone or with 0.2–0.5 μM SRIF. Fluorescence measurements were performed on photoreceptor inner segments with a 40× 1.3 numerical aperture fluar objective, using an Attofluor-imaging system (Atto Instruments, Rockville, MD). Optical excitation was accomplished using 340 and 380 nm wavelengths with an emission at 510 nm. The intensity of the fluorescence was minimized to prevent dye bleaching during experiments. Fluorescence measurements were acquired using Attofluor Ratiovision software and graphed with Attograph and Sigma Plot. The Attofluor system was calibrated using high (1 μM) and low (Ca-free solution containing 1 mM EGTA), and the gray scale intensities were adjusted to avoid saturation. The

concentration of fura-2 in the calibration tests was 8.8 μM, similar to the 5–10 μM concentration of fura-2 AM used in the experiments.

Electrophysiology: slice preparation

The procedures for obtaining retinal slices were similar to those described by Lukasiewicz et al. (1994). Briefly, the eyes were enucleated and hemisected, and the cornea, lens, and iris were removed. The retina was transferred, vitreal side down, to a Millipore filter paper (0.22 μm pore) and then sectioned manually into 150- to 200-μm-thick slices, which were mounted in a chamber and superfused at 2 ml/min during the experiment.

Solutions

Whole-cell voltage-clamp recordings of K^+ currents were made using patch electrodes containing (in mM): K gluconate 100, $MgCl_2$ 2, HEPES 10, ATP 2, and GTP 0.1, adjusted to pH 7.3 with KOH. The bath solution contained (in mM): NaCl 100, KCl 3, $CaCl_2$ 2, $MgCl_2$ 2, and HEPES 10, adjusted to pH 7.6 with NaOH. To isolate Ca^{2+} currents, the K gluconate of the intracellular solution was replaced by equimolar CsCl, while tetraethylammonium (TEA, 20 mM) was added to the bath solution, replacing an equimolar amount of NaCl. No Ca^{2+} chelator was included in the intracellular solution used to record either K^+ or Ca^{2+} currents. Somatostatin-14 (Bachem Bioscience, King of Prussia, PA) was applied to the bathing solution through the superfusion system at concentrations of 0.1–0.5 μM. Rods and cones were identified by their shape and location and by their characteristic hyperpolarization-activated I_h current. In some experiments 3 mM CsCl was included in the bath solution to block I_h. To test for a possible involvement of G_i/G_o proteins in the somatostatin-induced response, the eyecups were incubated 16–20 hr in Ringer's solution containing 400 ng/ml pertussis toxin (PTX) at 7°C in darkness.

Recording procedures

Whole-cell voltage- and current-clamp recordings were obtained in a conventional way (Hamill et a1., 1981) using an Axopatch 200B amplifier. Recording pipettes were made from borosilicate glass tubing (1.2 mm outer diameter; 0.6 mm inner diameter). Electrode resistance was typically 5–8 MΩ in the bath solution. After seal rupture the series resistance (10–15 MΩ) was compensated (70–80%) by a standard circuit. Whole-cell K^+ and Ca^{2+} currents were typically <1 nA, and the voltage errors resulting from inadequate compensation were estimated to be at most 3–5 mV. The average input resistance for rods, estimated from the steady-state current induced by a 10 mV voltage step from −60 mV, was 1.0 ± 0.1 GΩ (n = 10). Currents were filtered at 1 kHz by a low-pass Bessel filter and were sampled at 5–10 kHz. The pClamp software package (Axon Instruments) was used for data acquisition and analysis. Summary data are presented as means ± SE. The statistical comparison between groups was made with paired t tests; the corresponding p values are given in the text. In voltage-clamp experiments the membrane potential usually was held at −70 mV.

RESULTS

Localization of SRIF and the sst_{2A} receptor

SRIF immunostaining was observed in widely spaced amacrine cells, whose perikarya are at the border of the inner nuclear layer (INL) and the IPL. Immunolabeled amacrine cell processes were distributed within two narrow strata: sublamina 1 at the border of the INL and the IPL and sublamina 5 at the border of the IPL and the ganglion cell layer (GCL) (Fig. 1*a*). Because the morphology of these cells resembled that of the dopaminergic amacrine cells in tiger salamander (Watt et al., 1988), we conducted double-labeling experiments and

determined that SRIF and tyrosine hydroxylase were found within two distinct cell populations (data not shown).

sst_{2A} receptor immunoreactivity was localized to both the inner and outer retina, including cell bodies in the photoreceptor layer, and to processes in both plexiform layers (Fig. 1*b*). sst_{2A}-immunoreactive photoreceptors with prominent staining throughout the inner segment and synaptic terminals were observed (Fig. 1*b*, *arrows*). sst_{2A} receptor immunoreactivity also was expressed by isolated rod and cone photoreceptors, with strong staining of the inner segments and synaptic terminals, similar to the staining pattern observed in retinal sections (data not shown).

sst_{2A}-immunoreactive bipolar and amacrine cell bodies also were noted in which immunostaining was characterized by a thin rim of immunoreactivity at, or adjacent to, the plasma membrane. A dense network of immunostained processes was present in the outer plexiform layer and in all laminae of the IPL (Fig. 1*b*). Diffuse immunostaining was observed in the GCL. Immunostaining was completely eliminated in sections incubated in antibody that was preadsorbed with 10^{-5} M sst_{2A} 361–369 (Fig. 1*c*)

Effect of SRIF on voltage-gated currents in photoreceptors

Characteristics of outward K^+ current in photoreceptors—In the retinal slice preparation, rods were stepped for 50 msec to depolarizing voltages between −60 and +40 mV in 20 mV increments from a holding potential of −70 mV (Fig. 2*A, left*). Outward current was reliably observed for voltage steps positive to −40 mV. The tail current reversal potential for the outward current recorded was near −75 mV (data not shown), which is positive to the equilibrium potential of K^+ of −88 mV, assuming that the intracellular concentration of K^+ was equal to that in the pipette. The current was blocked in the presence of 20 mM TEA (data not shown).

Effect of SRIF on I_K—To examine the effect of SRIF receptor activation on I_K, various concentrations of SRIF from 0.1 to 1 μM were applied to rods. Even at the holding potential of −70 mV, 0.5 μM SRIF induced a steady outward current of 16 ± 3 pA ($n = 3$). This steady current is not reflected in the current–voltage plots of I_K (Fig. 2), because it was subtracted as a baseline current. Exposure to SRIF progressively increased the I_K evoked by depolarizing pulses (Fig. 2*A, right*) compared with those recorded in control Ringer's solution (Fig. 2*A, left*). Partial recovery was observed after a 10–15 min wash in SRIF-free Ringer's solution (data not shown). The corresponding *I–V* relationships are illustrated in Figure 2*B*, showing that an increase in I_K amplitude is not accompanied by a shift of the current–voltage relation along the voltage axis (Fig. 2*B*, *inset*). The threshold dose at which SRIF increased I_K was near 0.1 μM, and the maximum effect was obtained at ~1 μM. In subsequent experiments, we used concentrations of 0.1–0.5 μM. The mean increase of I_K (at +30 mV voltage step) induced by 0.5 μM SRIF was 58 ± 13% ($n = 20$; $p < 0.001$). The effect of SRIF was observed after ~1 min of application and reached a maximum in 2–4 min. A dose–response function for SRIF could not be obtained on a single cell because of incomplete recovery of I_K, even after a 10–15 min wash in normal Ringer's solution. A similar enhancement of I_K by SRIF was observed in cones (0.5 μM SRIF; mean increase, 37 ± 8%; $n = 5$; $p < 0.001$). In separate experiments ($n = 3$) done in the absence of Cs^+ in the bath solution, we found that the hyperpolarization-activated current (I_h) was not affected by SRIF in the same cells that showed a substantial increase in I_K current (data not shown).

Previous studies indicate that, in salamander photoreceptors, depolarization activates at least two types of K^+ current: a delayed rectifier and a Ca^{2+}-dependent K^+ current $I_{K–Ca}$) (Barnes and Hille, 1989). We used charybdotoxin (CTX; 20 nM) to block $I_{K–Ca}$ (Knaus et al., 1994). This reduced the outward current evoked by a depolarizing step from −70 to 0 mV (Fig. 2*C*,

mean reduction, 36 ± 17%; $n = 3$). Thereafter the slice was superfused with a mixture of charybdotoxin and SRIF (500 nM), resulting in a 49 ± 19% increase in outward current (Fig. 2*C,D*), which is the same degree of enhancement noted without charybdotoxin treatment. Thus, on the basis of its kinetic and pharmacological characteristics we identify the SRIF-sensitive outward current (Fig. 2*A*) as a delayed rectifier K^+ current (I_K).

Previous studies in other preparations have demonstrated that the action of SRIF on voltage-gated K^+ and Ca^{2+} currents is sensitive to PTX, indicating the participation of a PTX-sensitive G-protein (White et al., 1991; Ishibashi and Akaike, 1995; Delmas et al., 1998). We found that in slices obtained from eyecups after a 16–20 hr incubation with PTX (400 ng/ml), I_K of either rods or cones was not augmented by SRIF (Fig. 3*a*). The mean change of peak I_K by SRIF in PTX-pretreated cells was −8 ± 7% ($n = 3$; $p > 0.1$). There were no significant differences in the *I–V* characteristics of the I_K current recorded in control Ringer's solution or in the presence of SRIF (Fig. 3*b*). The histogram of Figure 3*c* summarizes the data obtained in control and PTX-treated slices.

Another test of G-protein involvement was the addition to the pipette solution of GDP$_\beta$S (500 μM), a compound that blocks the G-protein-mediated effects of neurotransmitters on neuronal Ca^{2+} currents (Holtz et al., 1986). After rupturing the cell membrane, a period of 4–5 min was allowed to ensure adequate dialysis with GDP$_\beta$S. Inclusion of GDP$_\beta$S in the patch pipette substantially abolished the SRIF-induced enhancement of I_K. In many cases we observed even a slight reduction of I_K after exposure to SRIF. In the experiment illustrated in Figure 4*a*, I_K was first recorded in control Ringer's solution and then after a 4 min exposure to 0.5 μM SRIF. The corresponding *I–V* relationships are illustrated in Figure 4*b*. The mean change of I_K induced by exposure to SRIF in the presence of GDP$_\beta$S was −6 ± 10% ($n = 8$; $p > 0.1$). Figure 4*c* summarizes these results, which indicate that a G-protein is implicated in the cascade underlying a SRIF-induced enhancement of I_K in retinal photoreceptors.

SRIF reduces Ca^{2+} current in rods—Ca^{2+} currents were isolated from other voltage-gated currents using ion substitution and channel blockers and were recorded in rods and cones under whole-cell voltage clamp. From a holding potential of −70 mV, depolarizing pulses of 70 msec duration were applied from −60 to +60 mV, in 10 mV increments, using 20 mM Ba^{2+} as the current carrier. For depolarizing steps positive to −40 mV, rods responded with a sustained inward current, which was completely blocked by application of 100 μM Cd^{2+}, increased by 10 μM BAY K 8644, and reduced in the presence of 50 μM nifedipine (data not shown), indicating that the Ca^{2+} current is mediated by dihydropyridine-sensitive, L-type Ca channels. In general, the kinetic and voltage-dependent characteristics of the Ca^{2+} current were similar to those described previously for salamander photoreceptors (Bader et al., 1982; Barnes and Hille, 1989). Figure 5*a* illustrates a representative experiment in which Ca^{2+} current was evoked by a depolarizing step from −70 to 0 mV in control external solution (1), after a 1 min exposure to 0.2 μM SRIF (2), and 2 min after the washout of drug (3). The SRIF-induced reduction of Ca^{2+} current was accompanied by a slowing of its activation kinetics. In control solution the time constant of activation was 2.2 ± 0.3 msec ($n = 6$), increasing significantly ($p < 0.05$; $n = 6$) to 3.4 ± 0.3 msec in the presence of SRIF. SRIF (0.2 μM) reversibly reduced peak Ca^{2+} current in rods by 33 ± 3% ($n = 10$; $p < 0.05$). Figure 5*b* illustrates the steady-state *I–V* relationship of Ca^{2+} current recorded in control external solution (*open circles*), and in the presence of SRIF (*closed circles*). It shows that the reduction of peak current is not accompanied by a significant shift of the voltage dependence of the calcium current.

The time course of SRIF blockade was evaluated, using the following protocol. We applied 70 msec depolarizing pulses to a test potential of 0 mV from a holding potential of −70 mV

each 5 sec (Fig. 5*c*). In other experiments a voltage ramp (from −70 to +50 mV) was applied every 10 sec. After obtaining five to six stable sequential responses, SRIF-containing solution was perfused into the bath, and the recordings continued another 2–3 min. Figure 5*c* illustrates that the actions of SRIF on Ca^{2+} current developed relatively rapidly (<1 min) and complete recovery was observed within a 1–2 min wash in control external solution, unlike the incomplete recovery of I_K even after a 10–15 min wash.

SRIF enhances Ca^{2+} current in cones—Surprisingly, we found that in contrast to its inhibitory action on Ca^{2+} current in rods, SRIF enhanced I_{Ca} in cones. Figure 6 *A* illustrates an experiment in which a cone was held at a membrane potential of −70 mV, and depolarizing pulses were applied from −40 to +40 mV in 10 mV increments. A family of whole-cell Ca^{2+} currents was recorded in control Ringer's solution, in the presence of 0.5 μM SRIF and after a wash in control Ringer's solution. In the presence of SRIF, the peak Ca^{2+} current was increased by 40 ± 8% ($n = 5$; $p < 0.005$). Figure 6*B* illustrates the *I–V* characteristics that show that SRIF enhanced Ca^{2+} current more dramatically at negative voltage steps (e.g., at −30 mV compared with 0 mV), resulting in a shift of peak Ca^{2+} current toward negative potentials. The data of Figures 5 and 6 are summarized in the histogram of Figure 6*C* that illustrates that SRIF enhances I_{Ca} in cones but decreases I_{Ca} in rods.

The SRIF-induced inhibition of I_{Ca} is G-protein coupled—sst_{2A} receptors are coupled to G_i or G_o proteins in different systems (Law et al., 1991, 1993; Gu and Schonbrunn, 1997). Some forms of G-protein-mediated inhibition of Ca^{2+} currents by neuromodulators are voltage dependent, being relieved by strong depolarizations (Bean, 1989; Hille, 1994). For example, in hippocampal neurons, the SRIF-induced inhibition of an N-type Ca^{2+} current has been shown to be highly sensitive to PTX and to depolarizing prepulses (Ishibashi and Akaike, 1995). To test for the possible involvement of a G-protein in the SRIF-induced inhibition of I_{Ca}, we performed experiments on eyecups pretreated with 400 ng/ml PTX. We found that PTX attenuated the inhibitory action of SRIF on I_{Ca}. The mean inhibition of I_{Ca} by somatostatin in PTX-pretreated rods was 8 ± 2% ($n = 3$; $p > 0.1$), compared with the 33% reduction observed in untreated rods.

A G-protein-dependent inhibition of I_{Ca} by SRIF may be mediated via an intracellular second messenger system or by a direct membrane-delimited mechanism. G-protein-dependent inhibition of I_{Ca} has been found to use either pathway, depending on the neurotransmitter involved (Beech et al., 1991; Shapiro and Hille, 1993). We tested whether intracellular Ca^{2+} might serve as a second messenger by changing the pipette solution to one containing 0 Ca^{2+}/10 mM BAPTA. The mean reduction of I_{Ca} by SRIF in the presence of BAPTA was ~37% ($n = 3$), the same degree of inhibition observed in rods not treated with BAPTA (data not shown). We concluded that SRIF-induced inhibition of I_{Ca} in rods is not mediated via changes in intracellular $[Ca^{2+}]$.

Effect of SRIF on intracellular Ca^{2+} accumulation—We used Ca^{2+}-imaging techniques to examine whether SRIF altered a depolarization-induced elevation of $[Ca^{2+}]_i$ in isolated photoreceptor synaptic endings. In these experiments, 50–100 mM K^+ (substituted for an equivalent amount of NaCl) was used to depolarize the cells and to stimulate Ca^{2+} entry through voltage-gated Ca^{2+} channels. Exposure to elevated $[K^+]_o$ induced a sustained increase of $[Ca^{2+}]_i$ in the synaptic terminals of isolated rods and cones (Fig. 7*a,c*). This effect was substantially reduced (~80%) in the presence of nifedipine (50 μM) and completely blocked in the presence of Cd^{2+} (100 μM), indicating that elevation of intracellular $[Ca^{2+}]$ was caused by activation of voltage-gated L-type Ca^{2+} channels, although release of Ca^{2+} from intracellular stores may also have contributed to the Ca^{2+} signal (Krizaj and Copenhagen, 1998). We found that, in rods, SRIF (0.2–0.5 μM)

significantly reduced the $[Ca^{2+}]_i$ accumulation induced by high K^+ (Fig. 7*a*). The mean reduction of Ca^{2+} entry by 0.5 μM somatostatin was 55 ± 18% ($n = 5$; $p < 0.05$). In agreement with electrophysiological results, we noted that in cones, 0.5 μM SRIF enhanced intracellular Ca^{2+} accumulation induced by high K^+ (Fig. 7*c*). The mean increase of $[Ca^{2+}]_i$ by 0.5 μM SRIF in cones was 50 ± 15% ($n = 5$; $p < 0.05$). Figure 7, *b* and *d*, summarizes these data that show that SRIF differentially affects Ca^{2+} signals in rods and cones. In control experiments we observed that two pulses of 90 mM K^+ elicited approximately equal increases in $[Ca]_i$, when separated by the same 1–2 min used for the experiments illustrated in Figure 7 (data not shown). Second, it was found that preexposure to PTX abolished the SRIF-induced increase in $[Ca^{2+}]_i$ in cones (−4 ± 1%; $n = 4$; $p > 0.1$; data not shown). Those cells that still possessed synaptic terminals after isolation manifested the most extensive changes in intracellular Ca^{2+} induced both by high K^+ and SRIF, indicating that SRIF receptors and/or Ca^{2+} channels may be concentrated in the photoreceptor synaptic terminals (Bader et al., 1982).

DISCUSSION

Cellular distribution of SRIF-containing neurons and SRIF receptors in the vertebrate retina

SRIF immunoreactivity has been described in the retinas of a variety of cold-blooded and homeotherm vertebrates (for review, see Brecha, 1983). The SRIF-containing cells are inner retinal neurons, typically amacrine or interplexiform cells (Yamada et al., 1980; Li et al., 1986; Smiley and Basinger, 1988; Rickman et al., 1996), with perikarya located either in the GCL or at the border of the INL and IPL. SRIF-containing neurons in mammals often are displaced amacrines, i.e., with cell bodies in the GCL (Engelmann and Peichl, 1996; Rickman et al., 1996). The retinal density of SRIF neurons is low [<100 cells mm^{-2} (Rickman et al., 1996)] in most parts of the retina but may reach a few thousand cells per square millimeter in restricted retinal regions (Engelmann and Peichl, 1996; Rickman et al., 1996). In spite of the low cellular density, SRIF processes create a continuous network in the IPL. Within the IPL the distribution of SRIF processes varies; in chicken retina, it is diffuse (Ishimoto et al., 1986), whereas in rabbit and salamander retinas, SRIF processes extend horizontally in laminae 1 and 5 of the IPL (Rickman et al., 1996) (present report). sst_{2A} receptors, on the other hand, are found in both the inner and outer retina (Johnson et al., 1998, 1999) (present report). The wider retinal distribution of SRIF receptors in relation to SRIF cells and processes indicates that SRIF reaches some targets by diffusion. Thus in general outline, the retinal SRIF system resembles closely that of the dopamine system (Witkovsky and Schutte, 1991), a resemblance that is heightened by the presumption that SRIF will affect synaptic transmission between rod and cone photoreceptors and second-order retinal neurons, as shown previously for dopamine (Witkovsky et al., 1988).

In the absence of antibodies against other forms of the SRIF receptors, we cannot conclude with certainty that the SRIF-induced physiological effects we have described were mediated by the sst_{2A} receptor, although this is a reasonable supposition because of the high density of sst_{2A} receptors on rod and cone terminals. The finding that these effects were blocked by PTX is not diagnostic, because all forms of SRIF receptor are reported to act via subtypes of either G_i or G_o proteins (Law et al., 1991; Takano et al., 1997), all of which are blocked by PTX.

SRIF-induced modulation of Ca^{2+} and K^+ currents in photoreceptors

K^+ current—Photoreceptors possess a mixture of voltage-dependent K^+ currents, including a delayed rectifier, I_K (Bader et al., 1982), a Ca^{2+}-dependent K^+ current, $I_{K–Ca}$ (Corey et al., 1984), and I_h, a mixed cation current (Fain et al., 1978; Barnes and Hille, 1989). Our data

indicate that SRIF selectively augments the delayed rectifier K^+ current. The enhancement of outward currents remained in the presence of charybdotoxin that blocks $I_{K–Ca}$, and it increased with depolarizing steps (Fig. 2) at which potentials I_h is inactivated (Akopian and Witkovsky, 1996). Exposure to SRIF also elicited a non-inactivating outward current that was 16 pA at the holding potential of −70 mV. This steady current is not attributable to I_h that has a reversal potential near −30 mV and so would generate an inward current at −70 mV. If the steady current were a leakage current, it would add a linear component to the total outward current, whose magnitude can be estimated by a regression line passing through E_K (−88 mV) and 16 pA at −70 mV. Because this putative current was not observed (Fig. 2), we conclude that the action of SRIF on K current is mediated primarily by I_K in salamander rods and cones.

The SRIF-induced steady K^+ current would be expected to hyperpolarize photoreceptors. At the resting potential of the photoreceptor in darkness (−40 mV) and with a value of 100 MΩ resistance to ground for rods in an intact retina (Owen and Copenhagen, 1977), photoreceptors will be hyperpolarized 1 mV for each 10 pA of steady current.

We noted that the SRIF-induced increase in I_K was blocked by PTX and by GDP$_\beta$S, consistent with the general finding that SRIF acts via PTX-sensitive G-proteins (Law et al., 1991; Rens-Domiano and Reisine, 1992). Our data agree with the demonstration by Wang et al. (1989) that in rat neocortical neurons, the enhancement by SRIF of a delayed rectifier current was antagonized by PTX. Takano et al. (1997) found that K_{ir} was activated by SRIF via $G_{\alpha i}$ 1 or 2 proteins, and Gu and Schonbrunn (1997) showed that the sst_{2A} receptor complexed specifically with $G_{\alpha i}$ 1–3 proteins, all of which are PTX-sensitive. Thus our data are consistent with the hypothesis that they were mediated by the sst_{2A} receptor that rod and cone photoreceptors express (Fig. 1), but a more compelling proof would require showing that SRIF receptors other than the sst_{2A} subtype are absent on salamander photoreceptors.

Ca^{2+} currents—The Ca^{2+} currents of salamander rods and cones have been investigated intensively (Bader et al., 1982; Corey et al., 1984; Barnes and Hille, 1989; Wilkinson and Barnes, 1996). They are of the L-type (dihydropyridine-sensitive, high voltage-activated, and nondesensitizing). Studies in several systems show that L-type currents are reduced by SRIF in a rapid and reversible manner (Ikeda and Schofield, 1989; Dryer et al., 1991; Shapiro and Hille, 1993; Ishibashi and Akaike, 1995). Our data on the fast, reversible inhibition of I_{Ca} in rods by SRIF and the independence of SRIF-induced effects on changes in intracellular [Ca^{2+}] suggest that the SRIF-induced inhibition of I_{Ca} is mediated by a membrane-delimited pathway. This possibility is consistent with the demonstration by Delmas et al. (1998) that a $G_{\beta\gamma}$ unit underlies the inhibition, by noradrenaline and SRIF, of an N-type Ca^{2+} current in rat sympathetic neurons.

The finding that the I_{Ca} of cone photoreceptors is enhanced by SRIF is novel. The enhancement consisted of a shift toward negative voltage of the activation function. This shift will be functionally important for cones, because their operating range extends for 20–30 mV negative to the membrane potential of approximately −40 mV in darkness (for review, see Attwell, 1990). The voltage-clamp records of I_{Ca} in cones are buttressed by the data from Ca^{2+} imaging that show that SRIF augments the increase in $[Ca^{2+}]_i$. It is possible that the differential action of SRIF on rod and cone calcium currents indicate a difference in the underlying Ca channel. Wilkinson and Barnes (1996) classified the cone L-Ca channel as the D subtype on the basis of its pharmacological profile, but we are unaware of a comparable study on the rod Ca channel.

Significance for retinal function of SRIF-induced alterations in photoreceptor K^+ and Ca^{2+} currents

The photoreceptor synapse is unusual in that rods and cones release glutamate tonically in darkness. Light, by hyperpolarizing the photoreceptor, reduces the rate of glutamate release (for review, see Attwell, 1990). Because glutamate release by photoreceptors is a Ca^{2+}-dependent process, it requires a sustained, voltage-dependent Ca^{2+} current, in accord with the demonstration that rods and cones use an L-type Ca current to mediate transmitter release (Rieke and Schwartz, 1996; Schmitz and Witkovsky, 1997; Witkovsky et al., 1997). A growing number of studies document that transmitter release from photoreceptor terminals is subject to multiple sources of neuromodulation. These include pH (Barnes et al., 1993), possibly related to GABA release by horizontal cells (Verweij et al., 1996), dopamine (Stella and Thoreson, 1998), and Ca release from intracellular stores (Krizaj et al., 1999).

SRIF will contribute to the overall modulation by downregulating glutamate release from rods via two mechanisms. The steady outward K^+ current will hyperpolarize the rod. Even a small (1–2 mV) hyperpolarization might be important, because of the change of slope of the Ca^{2+} current activation function that occurs near the −40 mV resting potential of the rod in darkness (Rieke and Schwartz, 1996; Witkovsky et al., 1997). Second, by further reducing I_{Ca} directly, glutamate release by rods will be attenuated.

The situation for cones is complex in that the shift toward negative voltages of the Ca^{2+} current–voltage function by SRIF will tend to be counterbalanced by any hyperpolarization resulting from a SRIF-induced increase in I_K. Thus a good test of the net action of SRIF on photoreceptor signaling will be to examine rod and cone inputs to the second-order retinal neurons and horizontal and bipolar cells. In amphibian retinas these second-order neurons receive a mixed input from rods and cones (Hare et al., 1986). On the basis of the findings of the present study, one would expect SRIF to reduce rod input and increase cone input, just as has been reported for the action of dopamine on amphibian horizontal cells (Witkovsky et al., 1988).

Acknowledgments

This work was supported by National Institutes of Health Grants EY 03570 to P.W., EY 07026 to J.J, and EY 04067 to N.B. and by a Veterans Administration Career Scientist award to N.B. Additional support came from the Hoffritz Foundation and an unrestricted grant from Research to Prevent Blindness to the Department Ophthalmology, New York University School of Medicine.

References

Akopian A, Witkovsky P. D2 dopamine receptor-mediated inhibition of a hyperpolarization-activated current in rod photoreceptors. J Neurophysiol. 1996; 76:1828–1835. [PubMed: 8890295]

Attwell D. The photoreceptor output synapse. Prog Retin Res. 1990; 9:337–362.

Bader CR, Bertrand D, Schwartz EA. Voltage-activated and Ca^{2+}-activated currents studied in solitary rod inner segments from the salamander retina. J Physiol (Lond). 1982; 331:253–284. [PubMed: 7153904]

Barnes S, Hille B. Ionic channels of the inner segment of tiger salamander photoreceptors. J Gen Physiol. 1989; 94:719–743. [PubMed: 2482325]

Barnes S, Merchant V, Mahmud F. Modulation of transmission gain by protons at the photoreceptor output synapse. Proc Natl Acad Sci USA. 1993; 90:10081–10085. [PubMed: 7694280]

Bean BP. Neurotransmitter inhibition of neuronal Ca^{2+} currents by changes in channel voltage dependence. Nature. 1989; 340:153–156. [PubMed: 2567963]

Beech D, Bernheim L, Hille B. Intracellular Ca buffers disrupt muscarinic suppression of Ca current and M current in rat sympathetic neurons. Proc Natl Acad Sci USA. 1991; 88:652–656. [PubMed: 1846449]

Boehm S, Betz H. Somatostatin inhibits excitatory transmission at rat hippocampal synapses via presynaptic receptors. J Neurosci. 1997; 17:4066–4075. [PubMed: 9151723]

Brecha, N. Retinal neurotransmitters: histochemical and biochemical studies. In: Emson, PC., editor. Chemical neuroanatomy. New York: Raven; 1983. p. 85-129.

Corey DP, Dubinsky JM, Schwartz EA. The calcium current in inner segments of rods from the salamander *(Ambystoma tigrinum)* retina. J Physiol (Lond). 1984; 354:557–575. [PubMed: 6090654]

Delfs, JR.; Dichter, MA. Somatostatin. In: Rogawski, MA.; Barker, JL., editors. Neurotransmitter actions in the vertebrate nervous system. New York: Plenum; 1985. p. 411-437.

Delmas P, Brown DA, Dayrell M, Abogadie FC, Caufield MP, Buckley NJ. On the role of endogenous G-protein beta gamma subunits in N-type Ca current inhibition by neurotransmitters in rat sympathetic neurons. J Physiol (Lond). 1998; 506:319–329. [PubMed: 9490860]

Dryer SE, Dourado MM, Wisgirda ME. Properties of Ca currents in acutely dissociated neurons of the chick ciliary ganglion: inhibition by somatostatin-14 and somatostatin-28. Neuroscience. 1991; 44:663–672. [PubMed: 1684410]

Engelmann R, Peichl L. Unique distribution of somatostatin-immunoreactive cells in the retina of the tree shrew (*Tupaia belangeri*). Eur J Neurosci. 1996; 8:220–228. [PubMed: 8713466]

Fain GL, Quandt FN, Bastian BL, Gerschenfeld HM. Contribution of a caesium sensitive conductance increase to the rod photoreceptors. Nature. 1978; 272:467–469.

Gu YZ, Schonbrunn A. Coupling specificity between somatostatin receptor sst2A and G proteins: isolation of the receptor-G protein complex with a receptor antibody. Mol Endocrinol. 1997; 11:527–537. [PubMed: 9139797]

Hamill OP, Marty A, Neher E, Sakmann B, Sigworth FJ. Improved patch clamp technique for high resolution current recording from cell and cell-free membrane patches. Pflügers Arch. 1981; 391:85–100. [PubMed: 6270629]

Hare WA, Lowe JS, Owen WG. Morphology of physiologically identified bipolar cells in the retina of the tiger salamander, *Ambystoma tigrinum*. J Comp Neurol. 1986; 252:130–138. [PubMed: 3793974]

Hille B. Modulation of ion-channel function by G-protein coupled receptors. Trends Neurosci. 1994; 17:531–536. [PubMed: 7532338]

Holtz GG, Rane SG, Dunlap K. GTP-binding proteins mediate transmitter inhibition of voltage-dependent calcium channels. Nature. 1986; 319:670–672. [PubMed: 2419757]

Hoyer D, Bell GI, Berelowitz M, Epelbaum J, Feniuk W, Humphrey PP, O'Carroll AM, Patel YC, Schonbrunn A, Taylor JE, et al. Classification and nomenclature of somatostatin receptors. Trends Pharmacol Sci. 1995; 16:86–88. [PubMed: 7792934]

Ikeda SR, Schofield GG. Somatostatin blocks a calcium current in rat sympathetic ganglion neurons. J Physiol (Lond). 1989; 409:221–240. [PubMed: 2479736]

Ishibashi H, Akaike N. Somatostatin modulates high-voltage-activated Ca channels in freshly dissociated rat hippocampal neurons. J Neurophysiol. 1995; 74:1028–1036. [PubMed: 7500129]

Ishimoto I, Millar T, Chubb IW, Morgan IG. Somatostatin-immunoreactive amacrine cells of chicken retina: retinal mosaic, ultra-structural features, and light-driven variations in peptide metabolism. Neuroscience. 1986; 17:1217–1233. [PubMed: 2872618]

Johnson J, Wong H, Walsh J, Brecha N. Expression of the somatostatin subtype receptor in the rabbit retina. J Comp Neurol. 1998; 392:1–9. [PubMed: 9482229]

Johnson J, Wu V, Wong H, Walsh JH, Brecha N. Somatostatin receptor subtype 2A in the rat retina. Neuroscience. 1999; 94:675–683. [PubMed: 10579559]

Katayama Y, Hirai K. Somatostatin presynaptically inhibits transmitter release in feline parasympathetic ganglion. Brain Res. 1989; 487:62–68. [PubMed: 2568871]

Knaus H-G, Eberhart A, Kaczorowski GJ, Garcia ML. Covalent attachment of charybdotoxin to the 2A β-subunit of the high conductance Ca^{2+}-activated K^{+} channel. J Biol Chem. 1994; 269:23336–23341. [PubMed: 7521879]

Krizaj D, Copenhagen DR. Compartmentalization of calcium extrusion mechanisms in the outer and inner segments of photoreceptors. Neuron. 1998; 21:249–256. [PubMed: 9697868]

Krizaj D, Bao JX, Schmitz Y, Witkovsky P, Copenhagen DR. Caffeine-sensitive calcium stores regulate synaptic transmission from retinal rod photoreceptors. J Neurosci. 1999; 19:7249–7261. [PubMed: 10460231]

Law S, Manning D, Reisine T. Identification of the subunits of GTP-binding proteins coupled to somatostatin receptors. J Biol Chem. 1991; 266:17885–17897. [PubMed: 1655730]

Law SF, Yasuda K, Bell GI, Reisine T. Gi alpha 3 and G (o) alpha selectively associate with the cloned somatostatin receptor subtype SSTR2. J Biol Chem. 1993; 268:10721–10727. [PubMed: 8098703]

Li HB, Lam DMK. Localization of neuropeptide-immunoreactive neurons in the human retina. Brain Res. 1990; 522:30–36. [PubMed: 1699634]

Li HB, Chen NX, Watt CB, Lam DMK. The light microscopic localization of substance P and somatostatin-like immunoreactive cells in the larval tiger salamander retina. Exp Brain Res. 1986; 63:93–102. [PubMed: 2426132]

Lukasiewicz P, Maple B, Werblin FS. A novel GABA receptor on bipolar cell terminals in the tiger salamander retina. J Neurosci. 1994; 14:1202–1212. [PubMed: 8120620]

Marc RE, Liu WL, Kalloniatis M, Raiguel SF, Van Haesendonck E. Patterns of glutamate immunoreactivity in the goldfish retina. J Neurosci. 1990; 10:4006–4034. [PubMed: 1980136]

Owen, WG.; Copenhagen, D. Characteristics of the electrical coupling between rods in the turtle retina. In: Barlow, HB.; Fatt, P., editors. Vertebrate photoreception. Academic; 1977. p. 169-192.

Rens-Domiano S, Reisine T. Biochemical and functional properties of somatostatin receptors. J Neurochem. 1992; 58:1987–1996. [PubMed: 1315373]

Rickman DW, Blanks JC, Brecha NC. Somatostatin-immunoreactive neurons in the adult rabbit retina. J Comp Neurol. 1996; 365:491–503. [PubMed: 8822184]

Rieke F, Schwartz E. Asynchronous transmitter release: control of exocytosis and endocytosis at the salamander rod synapse. J Physiol (Lond). 1996; 493:1–8. [PubMed: 8735690]

Rosenthal W, Hescheler J, Klaus-Dieter H, Spicher K, Trautwei W, Schultz G. Cyclic AMP-independent, dual regulation of voltage-dependent Ca currents by LHRH and somatostatin in pituitary cell line. EMBO J. 1988; 7:1627–1633. [PubMed: 2458919]

Schmitz Y, Witkovsky P. Dependence of photoreceptor glutamate release on a dihydropyridine-sensitive calcium channel. Neuroscience. 1997; 78:1209–1216. [PubMed: 9174087]

Schweitzer P, Madamba SG, Siggins GR. Somatostatin increases a voltage-insensitive K+ conductance in rat CA1 hippocampal neurons. J Neurophysiol. 1998; 79:1230–1238. [PubMed: 9497404]

Shapiro MS, Hille B. Substance P and somatostatin inhibit calcium channels in rat sympathetic neurons via different G protein pathways. Neuron. 1993; 10:11–20. [PubMed: 7678964]

Smiley JF, Basinger F. Somatostatin-like immunoreactivity and glycine high-affinity uptake colocalize to an interplexiform cell of the *Xenopus laevis* retina. J Comp Neurol. 1988; 274:608–616. [PubMed: 2906071]

Stella S, Thoreson WB. Differential modulation of rod and cone calcium currents by cAMP and a D2 dopamine receptor agonist. Invest Ophthalmol Vis Sci. 1998; 39:S983.

Sternini CH, Wong SV, Wu R, De Giorgio M, Yang J, Reeve NC Jr, Brecha N, Walsh J. Somatostatin 2A receptor is expressed by enteric neurons, and by interstitial cells of Cajal and enterochromaffin-like cells of the gastrointestinal tract. J Comp Neurol. 1997; 386:396–408. [PubMed: 9303425]

Takano K, Yasufuku-Takano J, Kozasa T, Nakajima S, Nakajima Y. Different G proteins mediate somatostatin-induced inward rectifier K+ currents in murine brain and endocrine cells. J Physiol (Lond). 1997; 502:559–567. [PubMed: 9279808]

Thoreson WB, Witkovsky P. Glutamate receptors and circuits in the vertebrate retina. Prog Retin Eye Res. 1999; 18:765–810. [PubMed: 10530751]

Vanetti M, Kouba M, Wang X, Vogt G, Hollt V. Cloning and expression of a novel mouse somatostatin receptor (SSTR2B). FEBS Lett. 1992; 311:290–294. [PubMed: 1397330]

Verweij J, Kamermans M, Spekreijse H. Horizontal cells feed back to cones by shifting the cone calcium-current activation range. Vision Res. 1996; 36:3943–3953. [PubMed: 9068848]

Wang HL, Bogen G, Reisine T, Dichter M. Somatostatin-14 and somatostatin-28 induce opposite effects on K^+ currents in rat neocortical neurons. Proc Natl Acad Sci USA. 1989; 86:9616–9620. [PubMed: 2574465]

Watt CB, Yang SZ, Lam DMK, Wu SM. Localization of tyrosine-hydroxylase-like-immunoreactive amacrine cells in the larval tiger salamander retina. J Comp Neurol. 1988; 272:114–126. [PubMed: 2898490]

White RE, Schonbrunn A, Armstrong D. Somatostatin stimulates Ca-activated K channels through protein dephosphorylation. Nature. 1991; 351:570–573. [PubMed: 1710783]

Wilkinson MF, Barnes S. The dihydropyridine-sensitive calcium channel subtype in cone photoreceptors. J Gen Physiol. 1996; 107:621–630. [PubMed: 8740375]

Witkovsky, P.; Dearry, A. A functional role of dopamine in the vertebrate retina. In: Osborne, NN.; Chader, C., editors. Progress in retinal research. Oxford: Pergamon; 1991. p. 247-292.

Witkovsky P, Schutte M. The organization of dopaminergic neurons in vertebrate retinas. Vis Neurosci. 1991; 7:113–124. [PubMed: 1931794]

Witkovsky P, Stone S, Besharse J. Dopamine modifies the balance of rod and cone inputs to horizontal cells of the *Xenopus* retina. Brain Res. 1988; 449:332–336. [PubMed: 3293703]

Witkovsky P, Schmitz Y, Akopian A, Krizaj D, Tranchina D. Gain of rod to horizontal cell synaptic transfer: relation to glutamate release and a dihydropyridine-sensitive calcium current. J Neurosci. 1997; 17:7297–7306. [PubMed: 9295376]

Yamada T, Marshak D, Basinger S, Walsh J, Moreley J, Stell W. Somatostatin-like immunoreactivity in the retina. Proc Natl Acad Sci USA. 1980; 77:1691–1695. [PubMed: 6103539]

Zalutsky RA, Miller RF. The physiology of somatostatin in the rabbit retina. J Neurosci. 1990; 10:383–393. [PubMed: 1968091]

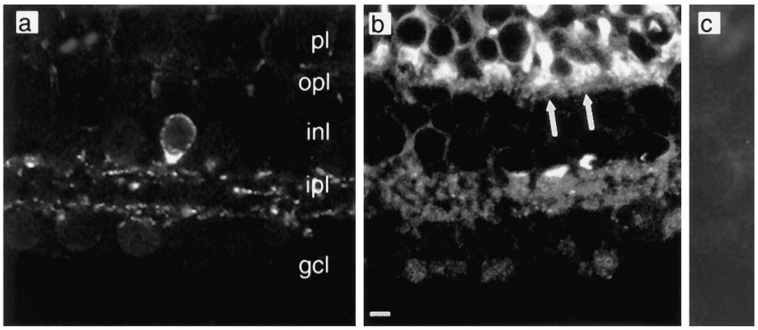

Figure 1.
Retinal distribution of SRIF and somatostatin sst_{2A} immunoreactivity. *a,* A SRIF-immunoreactive amacrine cell body whose processes extend into both distal and proximal portions of the IPL. *b,* sst_{2A} receptor immunoreactivity that is located in both plexiform layers. *Arrows* indicate positive staining of photoreceptor bases. *c*, Absence of sst_{2A} immunoreactivity when antibody was preabsorbed with a blocking peptide. *Labels* indicate retinal layers: *gcl*, ganglion cell layer; *inl*, inner nuclear layer; *ipl*, inner plexiform layer; *opl*, outer plexiform layer; and *pl,* photoreceptor layer. Scale bar: *a–c*, 5 μm.

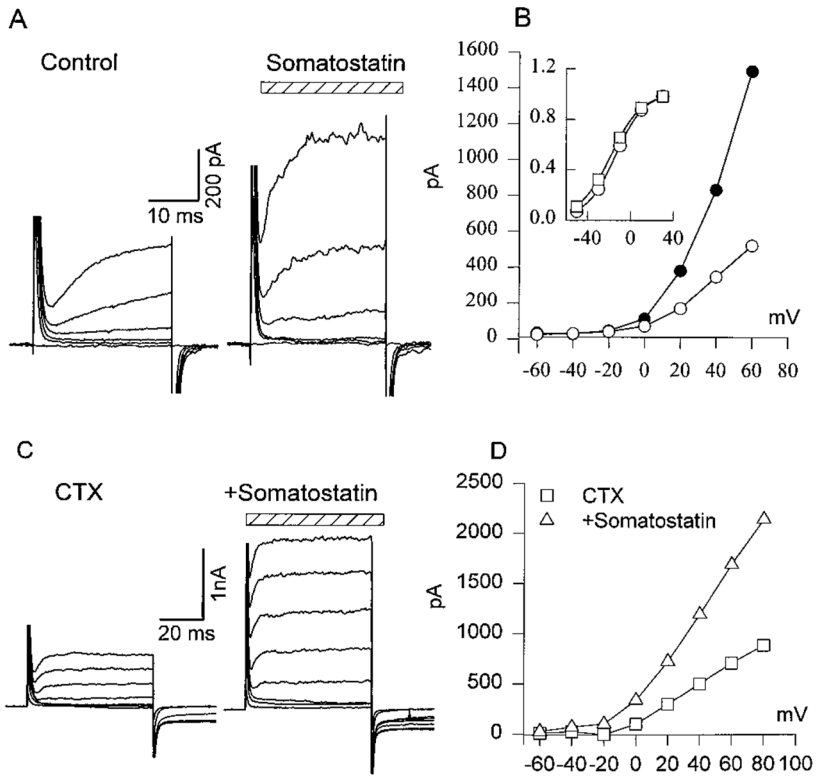

Figure 2.

Effect of SRIF on delayed outward K^+ current (I_K) in rods. *A,* SRIF increased voltage-activated K^+ current. I_K was evoked by holding cells at −70 mV and applying depolarizing steps from −60 to +40 mV in 20 mV increments in control external solution (*left*) and after a 4 min exposure to 0.5 μM SRIF (*striped horizontal bar; right*). *B, I–V* relationship of I_K obtained from the experiment described in *A* is shown. *Inset*, Somatostatin increased I_K amplitude without substantially changing the current–voltage relation. □, Control; ○, somatostatin. The *y*-axis of the *inset* is normalized current. *C*, CTX reduced outward currents (*left*) but did not prevent a somatostatin-induced increase in I_K. *D, I–V* relationship of outward current in the presence of CTX (□), or CTX + somatostatin (△); $n = 3$.

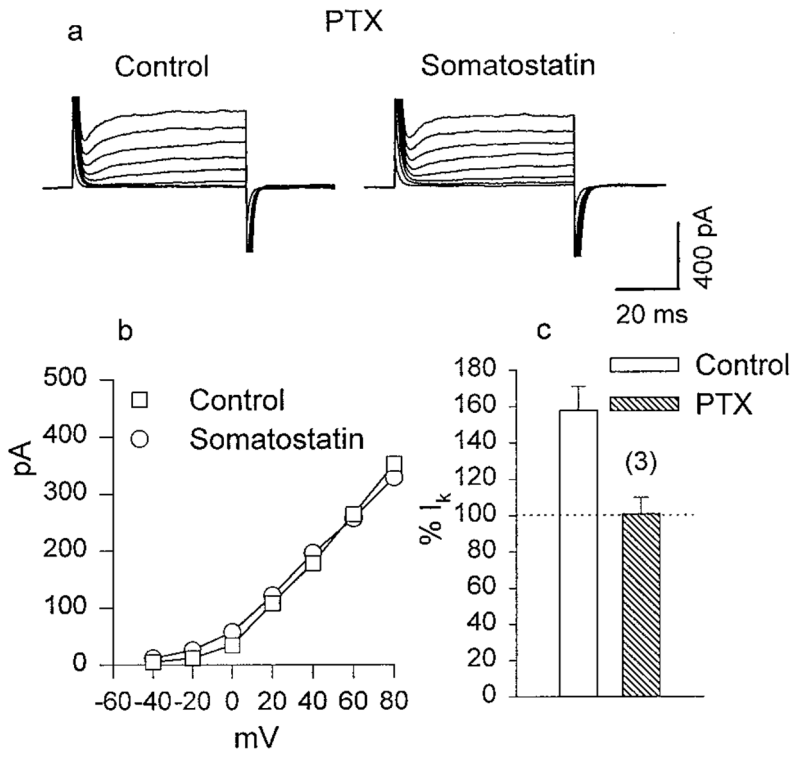

Figure 3.

Sensitivity to PTX of SRIF effect on I_K. By the use of a voltage protocol similar to that in Figure 2, a family of I_K currents was recorded in rods pretreated for 16–20 hr with PTX (400 ng/ml). *a*, Exposure to 0.5 μM SRIF for 5 min failed to enhance I_K. *b*, There was no significant difference in the *I–V* relationship of I_K recorded in control solution and in the presence of SRIF. *c*, The histogram summarizes the effects of SRIF on I_K in control and PTX-pretreated rods. *Numbers* in *parentheses* in this and subsequent figures are the sample size.

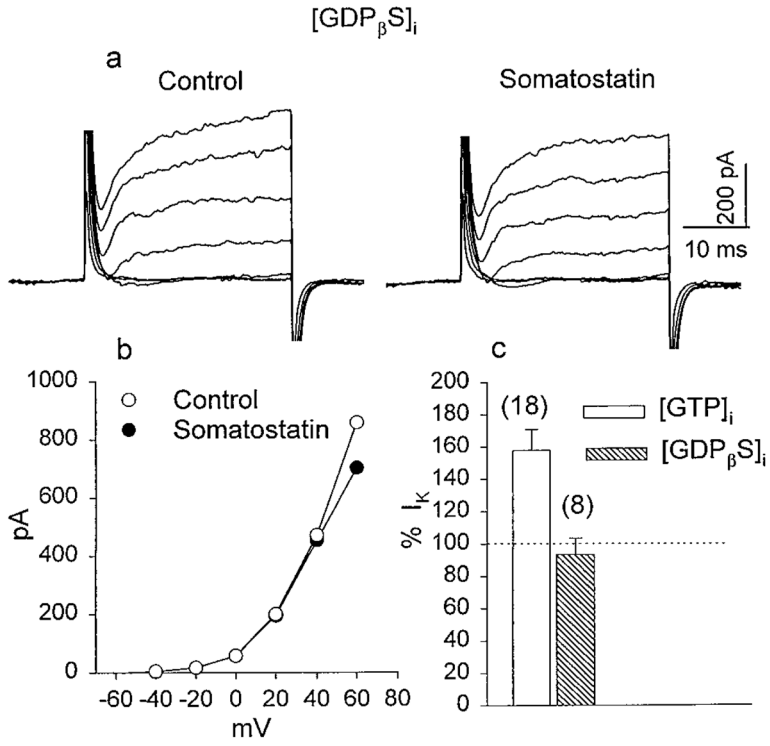

Figure 4.

The effect of GDP$_\beta$S on SRIF-induced changes in I_K. *a*, K^+ currents were recorded with a patch pipette containing 500 μM GDP$_\beta$S in control solution and after a 5 min exposure to 0.5 μM SRIF. *b*, The *I–V* relationship of I_K obtained from the experiments described in *a* indicates that SRIF failed to alter I_K in the presence of GDP$_\beta$S. *c*, The histogram summarizes SRIF-induced changes in I_K when the internal solution contained GTP (*open bar*) and when GTP was replaced by GDP$_\beta$S (*hatched bar*) to block G-protein activation.

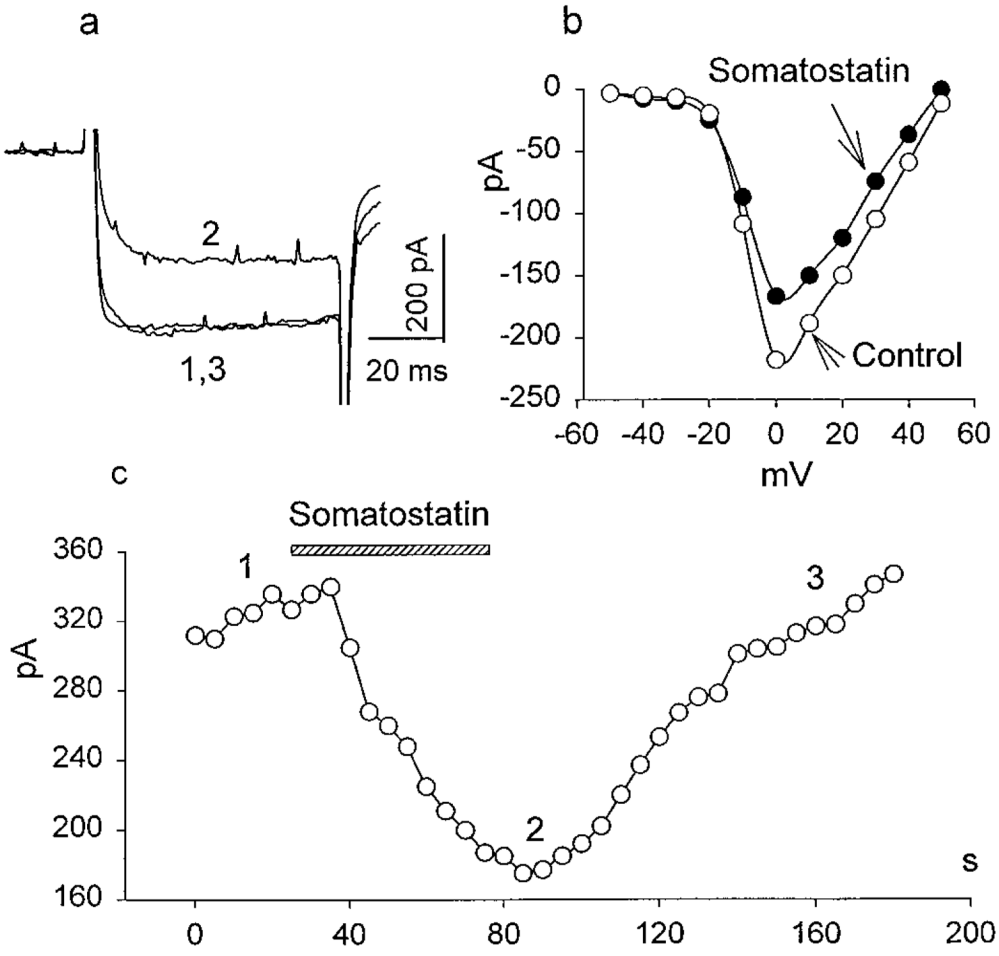

Figure 5.

The inhibitory effect of SRIF on high voltage-activated Ca^{2+} currents in rods. The test solution contained 0 $CaCl_2$ and 20 mM $BaCl_2$ substituted for equimolar NaCl. *a*, A depolarizing step to 0 mV from a holding potential of −70 mV was applied to record whole-cell Ca^{2+} current in control external solution (*1*), after a 1 min exposure to 0.2 μM SRIF (*2*), and after a wash (*3*). *b*, The *I–V* relationship of Ca^{2+} currents evoked by depolarizing voltage steps from −50 to +50 mV in 10 mV increments in the absence (*open circles*) and the presence of 0.2 μM SRIF (*closed circles*) is shown. *c*, The time course of SRIF blockade was evaluated by applying 70 msec depolarizing pulses to a test potential of 0 mV from a holding potential of −70 mV each 5 sec. The time of SRIF application is shown by the *hatched horizontal bar*. The *numbers* correspond to the *traces* in *a*.

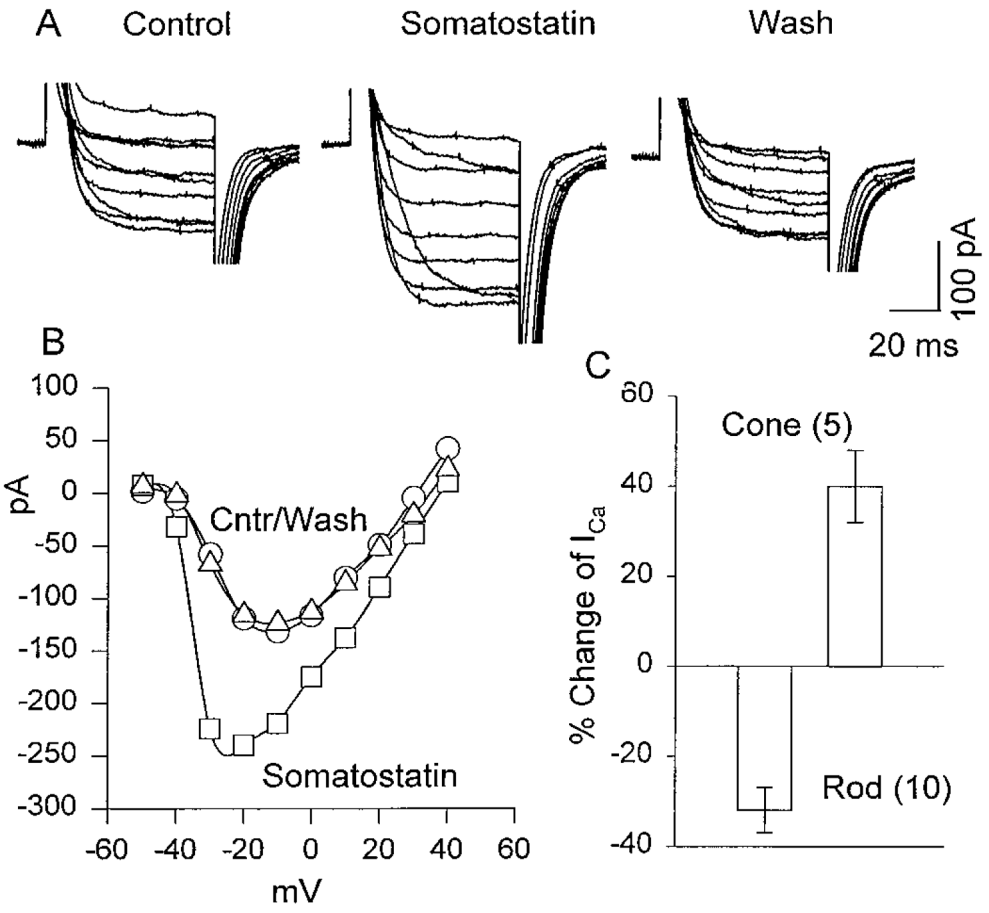

Figure 6.

Excitatory effects of SRIF on the Ca^{2+} current in cones. *A*, Cones were held at −70 mV, and depolarizing pulses were applied from −40 to +40 mV in 10 mV steps. Responses were recorded in 20 mM Ba solution as described for Figure 5. *Left*, In control Ba Ringer's solution. *Middle,* In 0.5 μM SRIF. *Right*, After a wash in Ba Ringer's solution. *B*, Current–voltage plot of the data in *A* is shown. *C*, A summary of the changes induced in the peak Ca current of rods and cones by SRIF is shown. *Cntr*, Control (○), wash (△).

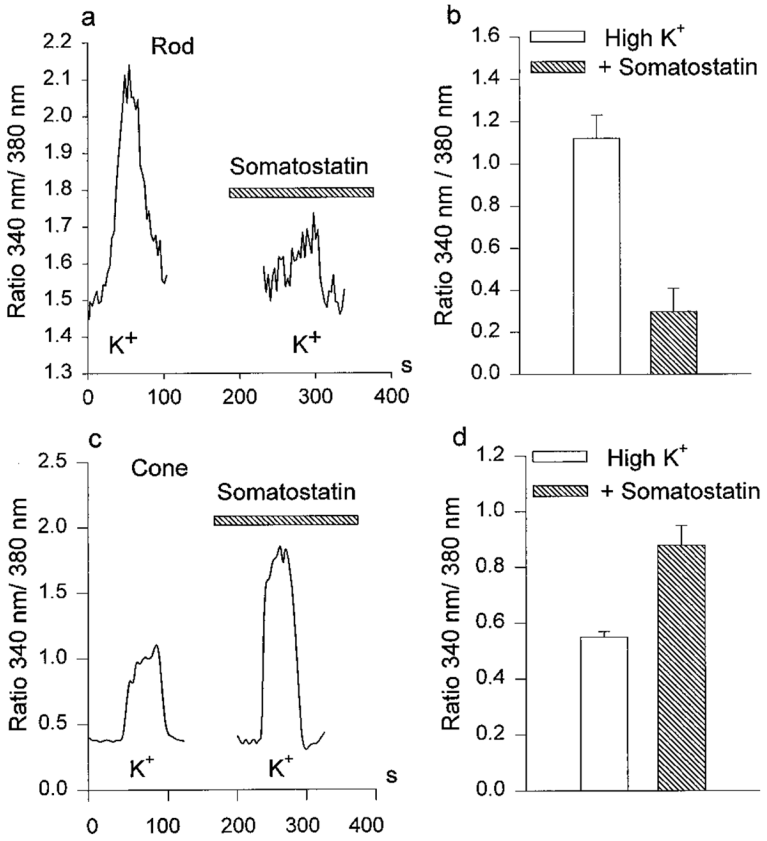

Figure 7.

Effects of somatostatin on K^+-induced Ca^{2+} accumulation in rods and cones. *a, c*, KCl (100 mM) was used to stimulate Ca^{2+} entry in the absence and the presence (*hatched horizontal bar*) of 0.5 μM somatostatin in rods (*a*) and cones (*c*). Somatostatin reduced Ca^{2+} accumulation in rods but increased it in cones. *b, d*, Histograms summarize the somatostatin-induced inhibition of Ca^{2+} accumulation in rods (*b; n* = 5) and its enhancement in cones (*d; n* = 5). *Vertical bars* show the mean values ± 1 SE.